Eur. Phys. J. B **42**, 407–414 (2004)
DOI: 10.1140/epjb/e2004-00397-0

THE EUROPEAN PHYSICAL JOURNAL B

Local waiting times in critical systems

L. Laurson and M.J. Alava[a]

Helsinki University of Technology, Laboratory of Physics, P.O. Box 1100, FIN-02015 HUT, Finland

Received 24 December 2003 / Received in final form 13 September 2004
Published online 23 December 2004 –

Abstract. The quiet times at a fixed point in space are investigated in a system close to or at a non-equilibrium phase transition. The statistics for such first-return times follow from the universality class of the dynamics and the ensemble: for a power-law waiting time distribution the exponent depends on the dimension and the underlying model. We study the two-dimensional Manna sandpile, with both the continously driven self-organized version and the tuned one. The latter has an absorbing state or depinning phase transition at a critical value of the control parameter. The connection to a driven interface in a random medium gives the exponent of the waiting time distribution. In the open ensemble, differences ensue due to the spatial inhomogeneity and the properties of the driving signal. For both ensembles, the waiting time distributions are found to exhibit logarithmic corrections to scaling.

PACS. 05.70.Ln Nonequilibrium and irreversible thermodynamics – 05.40.-a Fluctuation phenomena, random processes, noise, and Brownian motion – 52.25.Fi Transport properties

1 Introduction

Statistical behavior described by power-laws is appealing to attribute to the existence of "criticality" in the underlying dynamics. In the statistical mechanics sense, this means the proximity of a phase transition, and one of the prominent ideas in this respect is "self-organized criticality" (SOC). This is usually taken to mean that – whatever the exact definition of SOC – no fine-tuning to a critical point in the classical sense is needed and the system at hand is driven to such a critical state [1–4].

Within the physics of laboratory and space plasmas, dynamics of the solar wind and the magnetosphere and the sun there is much evidence for time-series exhibiting such critical signatures. One of the quantities that one may consider in this context is the *waiting time* of an experimental or observational parameter. This is defined in the most strict sense as the quiet or dead time intervals in which the measured signal is zero, but can also be considered after e.g. spatial or temporal thresholding. Examples are given by the local particle flux in the perimeter of a fusion device, and by satellite measurements of the solar wind [5–13].

The purpose of this paper is to consider waiting-time statistics at a single point $\vec{x}$ in a system exhibiting criticality. It is an essential point whether one has data for a "global" quantity or local statistics as considered here. In particular for classical SOC systems, with uncorrelated driving, global waiting time statistics are described most often by a Poisson process [14]. Recently it has been observed that for instance the magnetosphere is driven by a *correlated* signal, the flux of the solar wind, which implies that in order to make definite conclusions one has to understand both the underlying dynamics of the system, and the properties of the drive (input) [15].

The local waiting time statistics can follow a power-law probability distribution in a variety of cases though the global waiting times are Poissonian. This quantity, a series of waiting times t_w recorded at a specific location $\vec{x}$, is also perhaps easier to observe experimentally than the one that would describe a whole system. The source for the critical behavior for the probability distribution $P_w(t_w, \vec{x})$ is the avalanche dynamics in the systems, bursts of activity that are localized in space and time.

We consider the waiting times t_w which separate two consequent instances of time t_1 and t_2 ($t_w = t_2 - t_1$), between which the *activity* at $\vec{x}$ $\rho(\vec{x}, t) = 0$. Such waiting times result both from the quiescent periods during avalanches (internal waiting times $t_{w,i}$) and from the times it takes for an avalanche to nucleate at some point in the system from the external drive, and reach $\vec{x}$ (external waiting times $t_{w,e}$). This is illustrated in Figure 1. For both $t_{w,e}$ and $t_{w,i}$, one can consequently define separate distributions, $P_{w,e}$ and $P_{w,i}$.

The internal part, $P_{w,i}$, is possible to describe theoretically in models that give rise to interesting avalanche behavior. This is true in particular if such a model is related to non-equilibrium phase transitions: alternatively absorbing state transitions with a conserved quantity or depinning/pinning transitions of interfaces in disordered media [17–21]. These provide with a framework in terms of continuum equations and exponents describing the critical quantities at the critical point *with tuning*. Ensembles

[a] e-mail: mja@fyslab.hut.fi

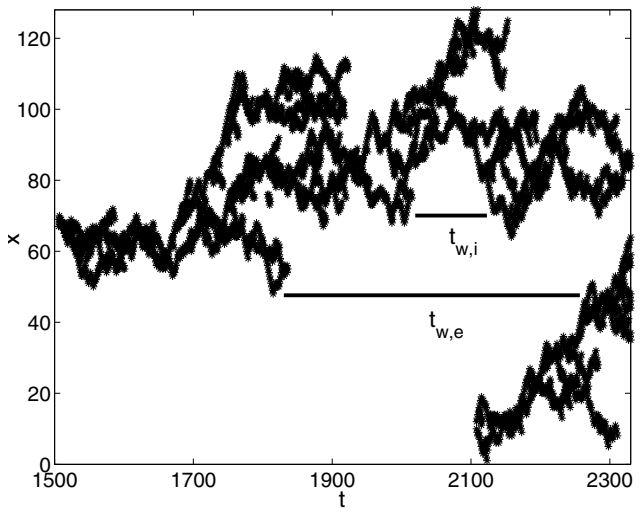

Fig. 1. An one-dimensional snapshot of a driven Manna model, and the definitions of the quantities.

where SOC arises are attained by introducing dissipation (open boundaries in typical sandpile models) and matching that with a slow drive. In the presence of both temporal and spatial statistical translation invariance waiting times are inherently related to the (self-affine) critical dynamics and can in general be described with the aid of the two-point temporal correlations, in the case of Markovian dynamics in particular. This also points out that the waiting times are related to the concept of persistence, which has been recently studied experimentally and theoretically [22]. In the case of "SOC" it is *not a priori clear* whether an effective description in terms of two-point correlations is available, due to the breakdown of spatial uniformity in the dynamics, and if so how the spatial aspects should be incorporated.

In the following we explore out of many possible models the two-dimensional Manna sandpile model [23], and study the waiting time distributions. Using such a sandpile is convenient since one can easily define two ensembles. First, there is the SOC one, which can be considered with finite drive rate f (grains added per unit time). This enables us to move from the pure SOC case (avalanches well separated) to a regime where the avalanches start to overlap [24,25]. Second, one can prepare the system with a fixed number of grains n which defines a control parameter $F = n/L^2$ (this is usually called the fixed energy ensemble, FES, in the absorbing state transition language) [26]. As F is varied, there is a phase transition between a phase where the average activity $\langle\rho\rangle$ is zero, and another one where it is finite. The transition turns out to be a depinning transition if one considers the integrated activity of the sandpile: this obeys an equation of motion which is reminiscent of an elastic object in a quenched force landscape [4,18,27]. At this critical point the order parameter – interface velocity ($\langle\rho\rangle$) – vanishes as the driving force F is tuned at F_c. The differences between the depinning/FES and the SOC ensembles are that 1) in the former one has to tune F to F_c, precisely, and 2) the SOC ensemble lacks translational invariance in $\vec{x}$.

Our main conclusion is that the waiting-time statistics reflects as expected the nature of the underlying phase transition: the dimension and the universality class. However, there are several twists that relate, here, to corrections to scaling in the 2d Manna model, and to the specific character of the SOC state compared to the usual phase transition. The structure of this paper is as follows. Section 2 explains the models and the quantities related to the critical behavior. Section 3 contains a scaling analysis of the waiting time distribution and numerical comparisons. Finally Section 4 finishes the paper with a discussion.

2 Criticality in sandpiles and interfaces

In the numerics to follow we consider the Manna sandpile model, defined via an integer state variable $z(x,t)$: If $z > z_c \equiv 1$ a site topples and gives two grains to its nearest neighbors with the destination of each chosen randomly. The dynamics is parallel, i.e.. all active sites topple simultaneously. The Manna model is an example of a sandpile model that can be mapped to interface depinning. Consider the time-integrated *activity* $H(\vec{x},t) = \int^t \rho(\vec{x},t')dt'$. This maps into the discrete Quenched Edwards-Wilkinson equation (QEW) or Linear Interface Model (LIM), in the form

$$\partial_t H = \theta(\nu\nabla^2 H + \eta(\vec{x},H) + F(\vec{x},t)) \qquad (1)$$

where the step-function θ forces the interface velocity to be either zero or unity [4,27]. The noise term η arises from the randomness in the toppling rules, and the F-term counts the number of grains added to the system. For a continuously driven system $F \sim ft$, which is compensated by the pinning at boundaries ($H = 0$) which corresponds to the loss of grains in the sandpile.

The continuum QEW has a a *depinning* (DP) transition at a F_c. This implies that the order parameter, the interface velocity, vanishes, and correlation functions show criticality typical of the QEW class with appropriate noise [19,20]. The self-affine temporal and spatial correlation functions are related to the critical exponent χ for the roughness, and z, the dynamical exponent. The QEW has an upper critical dimension of four (in 4+1 dimensions) with $\chi_{4d} = 0$, and $z_{4d} = 2$. The values of the exponents will in general depend on the exact character of the noise term η in the equation; strong correlations may change the scaling from the QEW one but the general trends are still such that the lower the spatial dimension d is, the larger the value of χ and the smaller the z.

Given the presence of only one length- and timescale, the depinning critical point has also the usual characteristic of kinetic roughening, that a roughening exponent $\beta_w \equiv \chi/z$ can be defined. This measures both the temporal two-point correlation function and the growth of fluctuations from a flat state. From the viewpoint of the avalanche structure and first-return properties the roughening exponent is important, since it relates to the steady-state (stationary) properties of the dynamics in the temporal domain. The fractal character of the spatiotemporal dynamics implies that if and when the first-return time

distribution $P_w(t_w)$ of the activity follows a power-law, $P_w(t_w) \sim t_w^{-\tau_w}$, the exponent has to relate to the integrated activity at a single location, which in turn follows from β_w [28,29]. Therefore we have that

$$\tau_w = 1 + \chi/z. \quad (2)$$

This would for the usual QEW class imply (using for simplicity and the sake of argument the 1-loop functional renormalization group results, instead of numerical values or 2-loop ones) that

$$\tau_{w,\mathrm{QEW}} \simeq 1 + [(4-d)/3]/[2 - 2(4-d)/9]. \quad (3)$$

It is a general fact that the dynamics of the system are reflected in the value of τ_w: For d small it will have a value closer to two, which gives an upper bound. For d approaching the upper critical dimension, τ_w gets closer to unity (with $\tau_w = 1$ at $d = 4$).

The above observation gives in other words strict limits to the waiting time distribution of an apparently critical system, whose dynamics are dictated by an underlying non-equilibrium transition with memory effects and (anomalously) diffusive dynamics (as $z \neq 2$). For the SOC ensemble the question now becomes, whether $\tau_{w,\mathrm{SOC}}$ agrees with the depinning estimate, and how properties of the drive might influence that. The normal QEW depinning transition is characterized by a cross-over to a thermal-noise system, with the waiting time distribution becoming trivial in the strong drive limit ($F \gg F_c$). For the finite-but-small drive SOC case, the system still has well-defined avalanches whose durations start to overlap while one may still consider the avalanches to exist separately. The question is, does the inhomogeneity caused by the open boundaries change the qualitative avalanche statistics?

3 Waiting time distributions

3.1 Fixed energy ensemble

First we consider the waiting times at the depinning (or fixed energy) critical point, $F_c(L)$. For the Manna model there are some direct results about β_w by Vespignani et al., and the FES scaling has been considered in great detail by later authors [26,30].

Figure 2 depicts the waiting time statistics as obtained at the critical point for four different system sizes. Even though for small t_w's there are clear deviations from power-law behaviour, it is possible to find a part in the $P_w(t_w)$ distributions for large t_w that can reasonably well be described by a power-law, a fit producing a waiting time exponent $\tau_w = 1.50 \pm 0.03$. One can try to further verify this by noticing that the large-t_w parts of the distributions from systems of different sizes L can be collapsed onto a single curve by using the scaling form

$$P_w(t_w, L) = t_w^{-\tau_w} \mathcal{P}\left(t_w/L^D\right) = L^{-D\tau_w} \tilde{\mathcal{P}}\left(t_w/L^D\right) \quad (4)$$

with $\tau_w = 1.52 \pm 0.03$ (and $D = 1.48 \pm 0.02$, Fig. 2), in good agreement with the value based on equation (2)

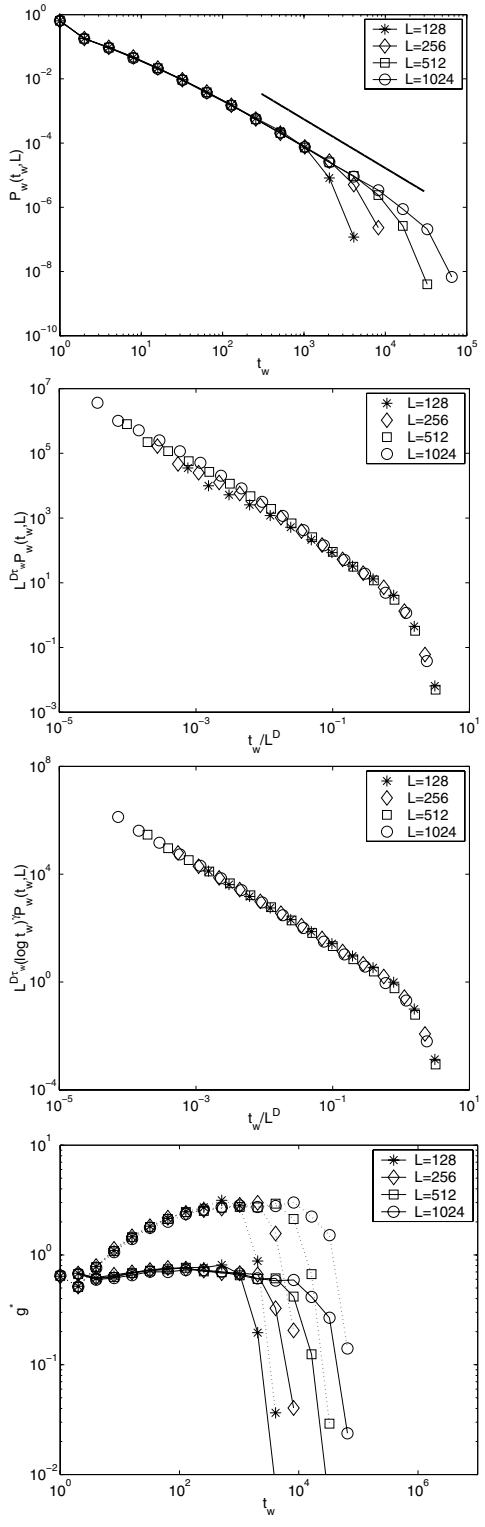

Fig. 2. Waiting time distributions in the FES/depinning case. The solid line corresponds to $\tau_w = 1.52$. In the first (upper) data collapse, $\tau_w = 1.52$ and $D = 1.48$. For the second collapse, showing the existence of logarithmic corrections, $\gamma = 0.74$ has been used, τ_w and D as above. The last panel demonstrates again that including logarithmic correction improves the fit, and that the exponent γ is seemingly independent of L. Points connected with solid line correspond to $\gamma = 0.74$, while those connected with dotted line have $\gamma = 0$.

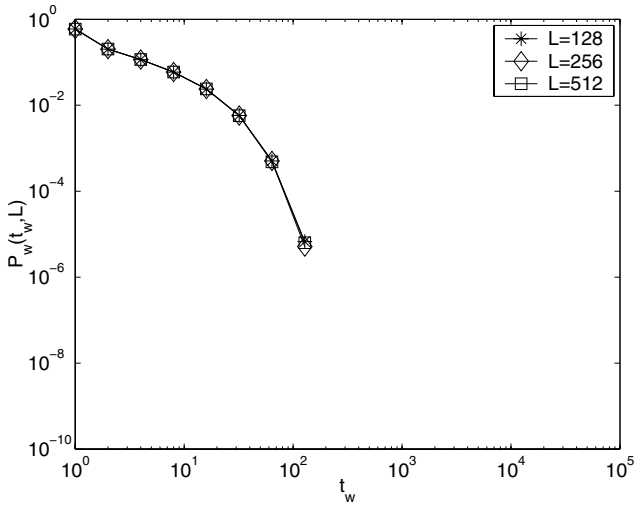

Fig. 3. An example of off-critical waiting time distributions in the depinning ensemble, $F = 1.1F_c(L)$.

and the result of reference [26], $\beta_w \sim 0.52$. Similar results can be obtained by analyzing the moments $\langle t_w^q \rangle$ of the $P_w(t_w)$-distribution [31]. One finds that these obey to a relatively good approximation scaling of the form $\langle t_w^q \rangle \sim L^{D(q-\tau_w+1)}$ with the exponents as found above.

Even though equation (4) works rather well for the largest waiting times, Figure 2 shows that such a simple ansatz is not appropriate for small t_w's. Therefore, inspired by a recent observation that the size and duration distributions of the Manna model exhibit *logarithmic corrections to scaling* [32], we try the scaling form

$$P_w(t_w, L) = L^{-D\tau_w} (\log t_w)^\gamma \tilde{\mathcal{P}} \left(t_w / L^D \right) . \qquad (5)$$

As Figure 2 demonstrates, this is clearly a better ansatz, describing well the whole range of waiting times with $\gamma = 0.74 \pm 0.05$. Notice that Dickman and Campelo studied the SOC ensemble; below we return to the differences and similarities of our numerical results to their conclusions. A pertinent point is that in our case a single value of γ applies to all L. This is demonstrated in the last panel of Figure 2, where we plot $g^* = t_w^{\tau_w} P_w / (\log t_w)^\gamma$ versus t_w for different system sizes.

In the off-critical situation (Fig. 3), on the other hand, large waiting times are cut-off due to the finite order parameter (activity $\langle \rho(\vec{x}, t) \rangle$ or velocity $\langle v(\vec{x}, t) \rangle$ for the history field) and the distributions become independent of the system size.

3.2 SOC ensemble

In this ensemble, open boundaries and the properties of the driving signal induce differences to the behaviour of the waiting time distribution. To inspect these effects systematically, we consider the distributions for different drive rates and locations, and dissect the distributions into the contributions coming from the internal and the external waiting times, as discussed earlier.

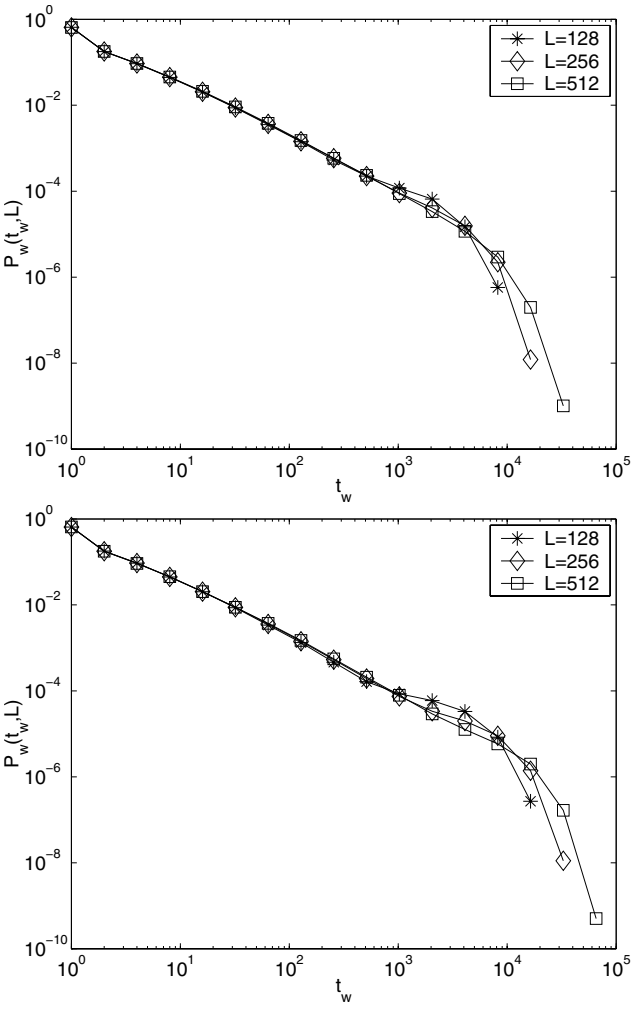

Fig. 4. Waiting time distributions in the finite-drive SOC ensemble for two different values of the drive rate, $f = 1/50$ (upper figure) and $f = 1/100$.

The finite-drive SOC case is illustrated in Figure 4 for a site *exactly in the center* of the SOC system. This choice of $\vec{x}$ is of special interest: one could expect it to resemble the depinning case as it is the only point in the system where there is no net flux of grains towards the boundaries. For any other $\vec{x}$ the boundary-induced effects will play a stronger role raising the question of SOC-ensemble-induced corrections to scaling. For the values of f used here new grains are added during the course of large avalanches, but since the drive takes place randomly in space it is usually so that the old avalanches and the new one do not overlap spatially (consider Fig. 1). The distributions have cut-offs that depend on both L and f. Even without a systematic analysis it is clear that choosing a smaller f will imply larger maximum waiting times, as is evident from the data.

It is instructive to compare the above finite-drive case to 1) a case where only internal waiting times, collected during the life-time of a single avalanche, are considered, and 2) the depinning case. Figure 5 shows distributions of the internal waiting times for a wide range of system

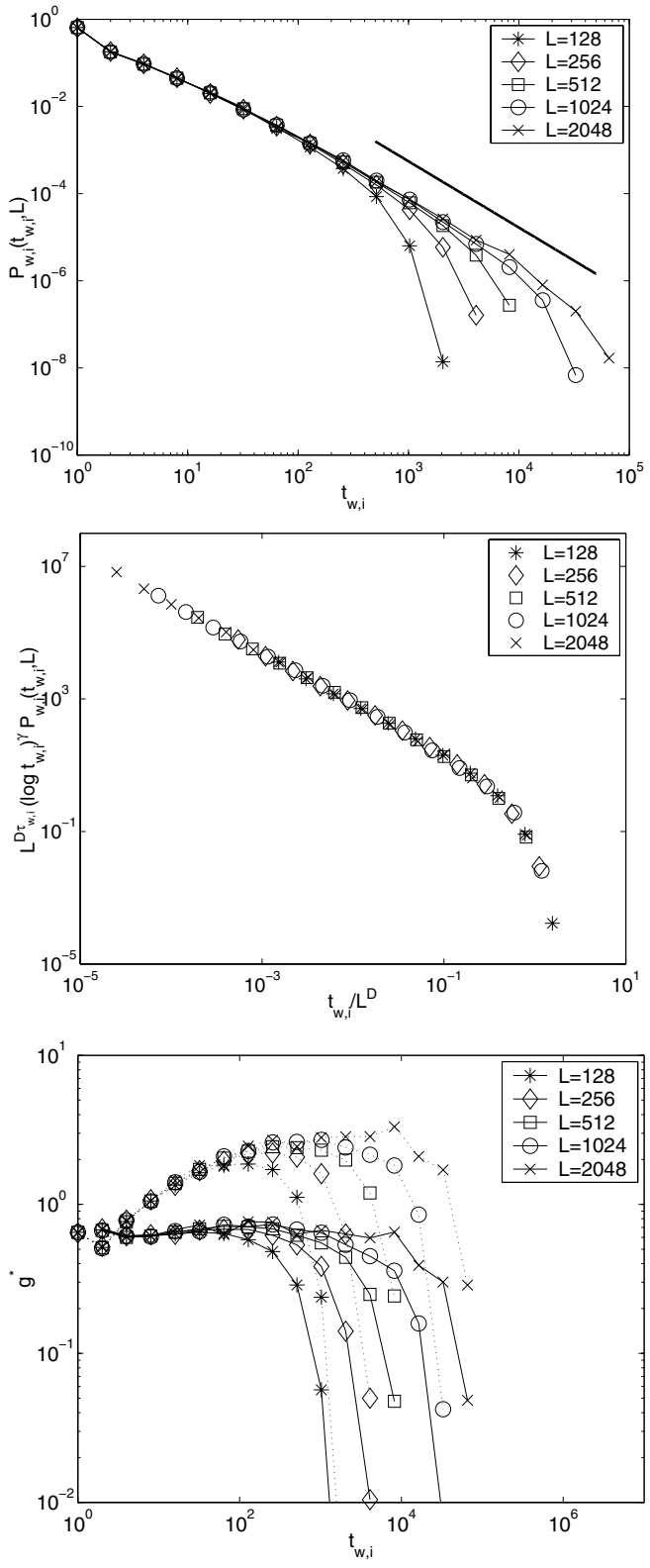

Fig. 5. Local internal waiting time distributions for a center site, SOC ensemble. The solid line corresponds to $\tau_w = 1.52$. In the data collapse, values $\tau_{w,i} = 1.52$, $D = 1.48$ and $\gamma = 0.74$ have been used. The last panel, where points connected with solid line have $\gamma = 0.74$ and those connected with dotted line $\gamma = 0$, demonstrates again that the exponent γ seems to be independent of L.

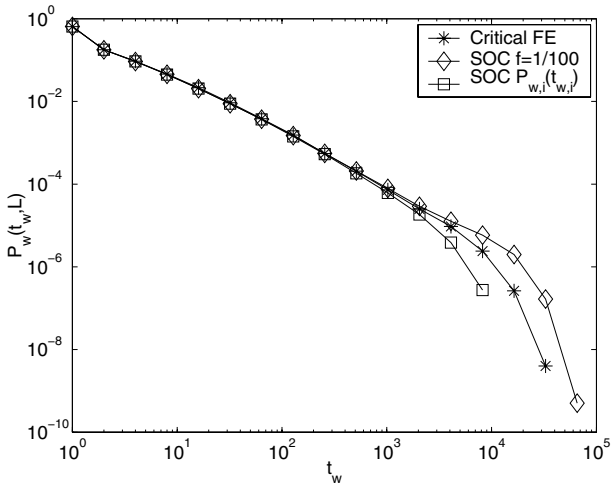

Fig. 6. A comparison, for $L = 512$, of the waiting times of the critical depinning (FE) and those of the center site in the SOC ensemble, (continuously driven and internal waiting times).

sizes. Interestingly, it seems to be possible to collapse the data by using the ansatz (5) with the *same parameters* as in the depinning case. In analogy with Figure 2, we also present the distributions using the scaling function $g^* = t_{w,i}^{\tau_{w,i}} P_{w,i}/(\log t_{w,i})^{\gamma}$. It is rather clear again that the same γ fits all the system sizes L. This is in slight contrast to reference [32] in which such exponents (for non-dissipative avalanches in particular) were found to be L-dependent. To this we have two comments to offer: first the quantity studied here is not avalanche duration nor size as in that case, and secondly note that the distribution is pre-conditioned with the choice that we look at the center of the system, only.

In Figure 6 we compare the 'raw data' for all the three cases for $L = 512$: Depinning ensemble, finite-drive SOC ensemble and internal waiting times in the SOC ensemble. It is noticeable that except for the cut-off behaviour, the three distributions are identical within the statistical uncertainty.

The comparison above has been attempted for a $\vec{x}$ that is as far from the boundaries as possible. Since the value of $\langle \rho(\vec{x}) \rangle$ is not uniform in the SOC case, it still remains to be seen how varying the measurement location would affect the statistics. As an extreme example, we consider the location $\vec{x} = (1, L/2)$ at the mid-edge of the system. Figure 7 gives the obvious conclusion that in the finite-drive case the relative amount of short (mostly internal) waiting times is smaller at the boundary than in the center site – at the edge the avalanches tend to dissipate grains and thus become extinct faster than elsewhere in the system. Furthermore, the long (typically external) waiting times are greater than in the center of the system, simply because the probability for an avalanche to reach a given edge site is on the average much smaller than to reach the center site and thus one has to wait longer before such an avalanche occurs. This can be further analyzed as follows: assume T grains are added to the system. If an avalanche dissipates at most $\mathcal{O}(1)$ grains, typically, a simple scaling argument about the dissipation profile gives that one

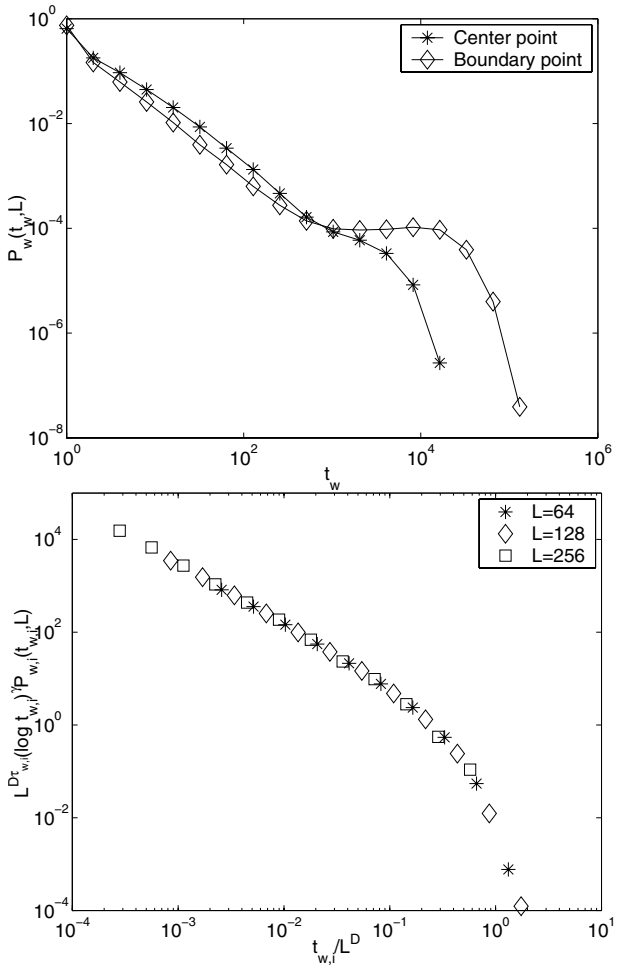

Fig. 7. SOC ensemble waiting time for two different locations (center of the system, at the (mid-)edge) for $L = 128$, $f = 1/100$ (upper panel). A data collapse for the waiting times at the edge of the system, with $\tau_{w,i} = 1.3$ and $D = 1.6$, without logarithmic corrections (lower panel).

grain reaches the center of the boundary for $3/8\ T/L$ (in our case) grains added, on the average. With $1/f = 100$ this implies, that the decay of the distribution should be located around $t \sim 3 \times 10^4$, in qualitative agreement with the data. However, a closer look at the internal waiting times at such boundary sites reveals, that the scaling is *not* the same: an attempt to use similar scalings ($\tau_w \sim 1.52$ with or without logarithmic corrections) fails and a better one is obtained with the particular values $\tau_w \sim 1.3$, $D \sim 1.6$, *without* logarithmic corrections.

The next question we address concerns the origin of the τ_w exponent for the SOC ensemble. Consider a special case in which the avalanches are *started* at the measuring point $\vec{x}$. These have a (perhaps $\vec{x}$-dependent) life-time distribution $P(t, \vec{x})$. If one now considers the internal waiting time distribution $P_{w,i}(t_{w,i}, \vec{x})$, this is a convolution over the waiting time distribution with a fixed life-time and $P(t, \vec{x}) \sim t^{-\tau_t}$ (ignoring the logarithmic corrections),

$$P_{w,i}(t_{w,i}, \vec{x}) = \int_{t_{w,i}}^{t_c(L)} P_w(t_{w,i}, t) P(t, \vec{x}) dt. \qquad (6)$$

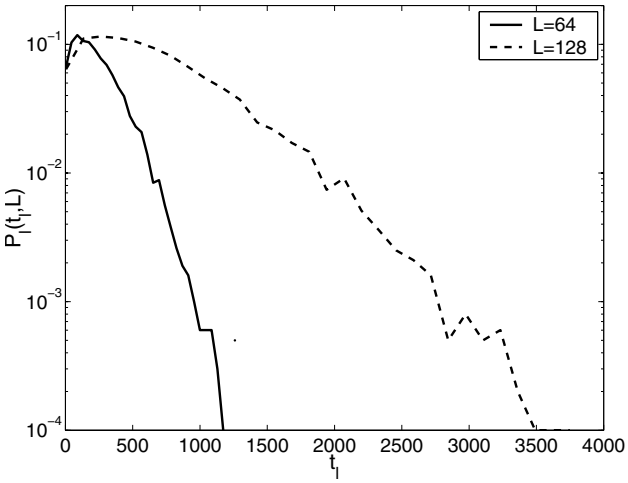

Fig. 8. Distribution of the life-time t_l a randomly started avalanche has left once it has reached the center site for the first time.

If the former of these two is just given as an assumption by the depinning critical point one, $P_w(t_{w,i}) \sim t_{w,i}^{-\tau_w}$, cut-off by t, one obtains that

$$P_{w,i}(t_{w,i}, \vec{x}) \sim t_{w,i}^{-\tau_w + 1 - \tau_t}. \qquad (7)$$

The case of the spatially randomly started avalanches (due to the spatially random driving signal), however, is different. Instead of the life-time distribution $P(t, \vec{x}) \sim t^{-\tau_t}$, one should now use the distribution $P_l(t_l, \vec{x})$ of the life-time t_l that an avalanche still has left once it has reached the measuring point for the first time. From Figure 8 one sees that in contrast to the power-law total life-time distribution, $P_l(t_l, \vec{x})$ for the center site decays exponentially. This is probably related to the fact that the distribution of first arrival times (or external waiting times) is also an exponential and given by the cut-off of the total life-time distribution – a typical avalanche has a more or less equal distance to travel both to the boundary and to the center site, the time it takes for it to propagate the former distance giving the cut-off scale of the $P(t)$-distribution. In case the use of $P_w(t_w) \sim t_w^{-\tau_w}$ in equation (6) is justified, one thus arrives at the conclusion that the exponent of the internal waiting time distribution *for a center site* in the SOC ensemble with spatially homogeneous random drive is in fact τ_w of the depinning case,

$$P_{w,i}(t_{w,i}, \vec{x}) \sim t_{w,i}^{-\tau_w}. \qquad (8)$$

This result is consistent with our simulations. We observe that the $P_{w,i}(t_{w,i}, L)$-distributions for the center site (Fig. 5) can be well described by equation (5), with τ_w having the depinning value $\tau_w \sim 1.52$.

Equations (7) and (8) suggest that the exponent of the $P_{w,i}(t_{w,i}, \vec{x})$-distribution can be affected by the spatial properties of the driving signal. Indeed, this effect can be seen in Figure 9, where we compare the distributions of waiting times with uniform drive and in the case where the avalanches are started at the measuring point only. The latter distribution seems to decay somewhat faster,

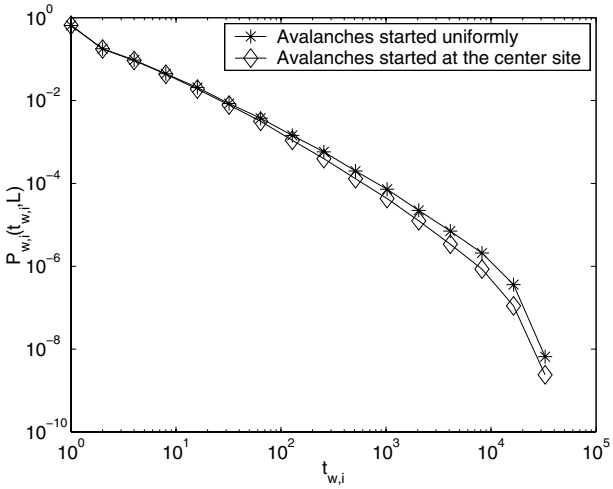

Fig. 9. Comparison of the internal waiting time distributions with two spatially different driving signals, $L = 1024$.

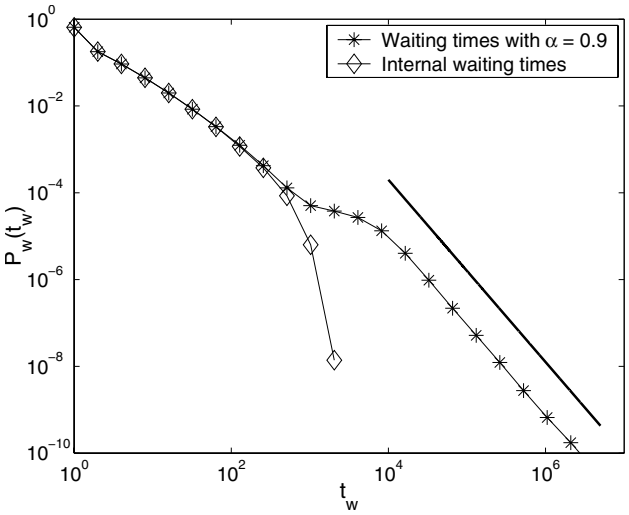

Fig. 10. The effect of power-law distributed drive rates (with $\alpha = 0.9$) on the waiting time distribution for $L = 128$. The solid line corresponds to an exponent 2.1, as predicted by equation (10).

as predicted by equation (7) (as $\tau_t > 1$), but we are unable to extract the precise value of the exponent from the data.

In addition to the spatial properties, one can also consider the effect of a temporally non-uniform driving signal to the waiting time distribution. Assume that the external waiting times $t_{w,e}$ are essentially due to a Poisson process with a slowly fluctuating drive rate f. Taking this to be a piecewise constant Poisson process with a large number of drive rates from some probability distribution $P_f(f)$, the probability distribution for external waiting times becomes

$$P_{w,e}(t_{w,e}) = \frac{1}{f_0}\int_0^\infty P_f(f) f^2 e^{-f t_{w,e}} df, \qquad (9)$$

where f_0 is the mean drive rate. By substituting into this, out of many possible distributions, a power-law distribution for the drive rates, $P_f(f) \sim f^{-\alpha}$, with a cut-off at some f_{max}, one obtains for long external waiting times

$$P_{w,e}(t_{w,e}) \sim t_{w,e}^{-(3-\alpha)}. \qquad (10)$$

In other words, in the presence of power-law distributed drive rates, one could expect to see a distribution for the local waiting times that has two distinct power-law regions. For t_w small, the distribution is dominated by the internal waiting times and should therefore be more or less unchanged, with the usual exponent τ_w. For larger values of t_w, where the external waiting times dominate, we have now power-law behaviour with an exponent $3-\alpha$, in contrast to the usual exponential behaviour. This procedure can also be applied to the usually exponential *global* waiting time distribution to get a power-law distribution for long global waiting times, which is essentially what has been done in reference [15] in the case of an exponential rate distribution. Figure 10 demonstrates this effect with $\alpha = 0.9$. In addition to the power-law distributed long (external) waiting times, one may observe that for t_w small, the distribution is seemingly independent of the temporal properties of the drive. We can thus conclude that in addition to the dependence on the measurement location $\vec{x}$, the waiting time distributions of the SOC ensemble may also depend in a rather complicated manner on both the spatial and temporal properties of the external driving signal.

4 Conclusions

We have studied the details of local waiting times in a sandpile model, to elucidate the origins of the probability distribution. For the system at hand, the two-dimensional Manna model, we are able to relate the internal waiting time exponent to the critical exponents of the phase transition of the same model, in the "fixed energy" or depinning ensemble. This works in spite of the fact that to reach the best collapse of the data we have to resort to corrections to the scaling function(s). It is maybe not surprising that the SOC case follows the FES/DP scaling so well since though the distribution does vary with the measurement location the agreement is found for a site at the center of the system. In any case, this result sheds further light on the debate as to when these two ensembles are equivalent, and if the SOC scaling exponents follow from the depinning phase transition [35]. It is interesting that the waiting time distributions seem to imply the presence of logarithmic corrections to the scaling function, as recently suggested by Dickman and Campelo in the case of the size and duration distributions, and very importantly this seems also to be the case for the "usual" phase transition.

A central point is that if the scenario is not complicated by other effects like a complicated driving, the existence of an underlying "continuum theory" fixes the range of exponents that can be expected. One particular case where this could be of interest is provided by so-called critical curvature models used to describe solar activity [9]: The continuum equation is different and the zoo of

possible exponents is yet not fully understood, but the basic outcome should be the same.

Understanding the local waiting times is based on the fact that the activity forms an effectively fractal pattern regardless of the ensemble and the point of observation. Complications would arise in the SOC case if the pattern of avalanches would have correlations, either spatial or temporal, due to the driving signal. This picture resembles to a large degree the case of Barkhausen noise, in systems with a finite field ramp rate, in the way the waiting time distribution changes as one moves away from the critical point. The study of a case with varying drive rates reveals that the effective exponent can be tuned. It would be interesting to consider scenarios like colored noise since with eg. a spatially correlated drive signal the avalanche overlap might complicate the outcome.

We finish by pointing out two different nuances. First, by considering the waiting times in a SOC system (with a non-zero or with a vanishing drive rate) we have simultaneously considered "persistence" or first-return characteristics in a SOC system. Its power-law features seem to be related as noted earlier to the translation-invariant ensemble, but understanding in detail the way the waiting times behave as a function of $\vec{x}$ would seem interesting. We have restricted ourselves to comparing the bulk and the very edge of a sandpile (or the center point and the outmost point of an interface in a random medium). The presence of logarithmic features in the scaling of $P(t_w)$ should also have consequences for the two-point correlation functions in this particular model; this is an open problem for future.

Second, the relative insensitivity of the waiting time exponent (limited to between one and two) means that the ensemble does not matter much, and therefore it seems a fruitful idea to try to establish observational or experimental limits to such exponents. This might make it possible to establish the effective nature of the underlying dynamics – the dynamical equation, the noise, and the dimensionality. Recent experiments on fusion plasma devices (tokamaks, stellarators, reverse field pinces) [33,34] have highlighted this matter. Recall that based on the scaling picture the waiting time exponent is bounded from above by two. The existence of experimental indications (for conditions that correspond in practice to a local measurement) for higher values in some cases implies in our opinion that the driving signal has temporal correlations.

We are grateful to the Center of Excellence program of the Academy of Finland for support.

References

1. D. Sornette, *Critical Phenomena in Natural Sciences* (Springer, Berlin, 2000)
2. H.J. Jensen, *Self Organized Criticality* (Cambridge Univ. Press, Cambridge, 1998); G. Grinstein, in *Scale Invariance, Interfaces and Nonequilibrium Dynamics*, NATO ASI, Ser. B: Physics, Vol. 344, edited by A. McKane et al. (Plenum, New York, 1995)
3. M.A. Muñoz, R. Dickman, R. Pastor-Satorras, A. Vespignani, S. Zapperi, Braz. J. Phys. **30**, 27 (2000)
4. M. Alava, `cond-mat/0307668`; in: *Advances in Condensed Matter and Statistical Mechanics*, edited by E. Korutcheva, R. Cuerno (Nova Science Publishers, 2004)
5. M.P. Freeman, N.W. Watkins, D.J. Riley, Phys. Rev. E **62**, 8794 (2000); M.S. Wheatland, P.A. Sturrock, J.M. McTiernan, Astrophys. J. **509**, 448 (1998)
6. M.S. Wheatland, Y.E. Livinenko, Solar Phys. **211**, 255 (2002)
7. D. Hamon, M. Nicodemi, H.J. Jensen, Astron. Astrophys. **387**, 326 (2002)
8. P. Grigolini, D. Leddon, N. Scafetta, Phys. Rev. E **65**, 046203 (2002)
9. J.P. Norman, P. Charbonneau, S.W. McIntosh, H.L. Liu, Astroph. J. **557**, 891 (2001)
10. S. Galtier, Solar Phys. **201**, 133 (2001)
11. F. Lepreti, V. Carbone, P. Veltri, Astroph. J. **555**, L133 (2001)
12. E. Spada et al., Phys. Rev. Lett. **86**, 3032 (2001)
13. S. Chapman, N. Watkins, Space Sci. Rev. **95**, 293 (2001)
14. R. Sánchez et al., Phys. Rev. Lett. **88**, 068302 (2002); R. Sánchez et al., Phys. Rev. E **66**, 036124 (2002)
15. M.S. Wheatland, Astrophys. J. **536**, L109 (2000)
16. N.W. Watkins, S. Oughton, M.P. Freeman, Plan. Space Sci. **49**, 1233 (2001)
17. R. Pastor-Satorras, A. Vespignani, Phys. Rev. E **62**, 5875 (2000); M. Rossi, R. Pastor-Satorras, A. Vespignani, Phys. Rev. Lett. **85**, 1803 (2000)
18. M. Alava, M. Muńoz, Phys. Rev. E **65**, 026145 (2002)
19. T. Nattermann et al., J. Phys. France II **2**, 1483 (1992); H. Leschhorn et al., Ann. Physik **7**, 1 (1997)
20. O. Narayan, D.S. Fisher, Phys. Rev. B **48**, 7030 (1993)
21. P. Chauve, P. Le Doussal, K. Wiese, Phys. Rev. Lett. **86**, 1785 (2001)
22. J. Krug et al., Phys. Rev. E **56**, 2702 (1997); J. Merikoski et al. Phys. Rev. Lett. **90**, 024501 (2003)
23. S.S. Manna, J. Phys. A **24**, L363 (1992); S.S. Manna, J. Stat. Phys. **59**, 509 (1990)
24. T. Hwa, M. Kardar, Phys. Rev. A **45**, 7002 (1992)
25. M. Alava, A.K. Chattopadhyay, Phys. Rev. E **69**, 016104 (2004)
26. A. Vespignani et al., Phys. Rev. E **62**, 4564 (2000)
27. M.J. Alava, K.B. Lauritsen, Europhys. Lett. **53**, 563 (2001)
28. N.-N. Pang, N.Y. Liang, Phys. Rev. E **56**, 1461 (1997)
29. M. Paczuski, S. Maslov, P. Bak, Phys. Rev. E **53**, 414 (1996)
30. S. Lübeck, Phys. Rev. E **66**, 046114, (2002); J. Kockelkoren, H. Chaté, `cond-mat/0306039`
31. C. Tebaldi, M. De Menech, A.L. Stella, Phys. Rev. Lett. **83**, 3952 (1999)
32. R. Dickman, J.M.M. Campelo, Phys. Rev. E **67**, 066111 (2003); `cond-mat/0301054`
33. R. Sánchez et al. Phys. Rev. Lett. **90**, 185005 (2003)
34. V. Antoni et al., Phys. Rev. Lett. **87**, 045001 (2001)
35. See e.g. [4,29]; A. Montakhab, J.M. Carlson Phys. Rev. E **58**, 5608 (1998); M.J. Alava, J. Phys.: Condens. Matter **14**, 2353 (2002); S. Lübeck, P.C. Heger, Phys. Rev. E **68**, 056102 (2003)